Asian Journal of Chemistry; Vol. 24, No. 9 (2012), 4205-4212

ASIAN JOURNAL OF CHEMISTRY

www.asianjournalofchemistry.co.in

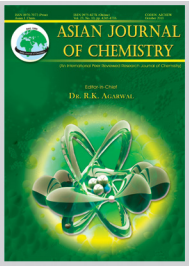

Optimization of Pore Structures and Supercapacitor Properties of Carbon Aerogel Electrodes†

CHANG-YEOUL KIM*, A. RUM JANG and KWANG YOUN CHO

NIT Convergence Center, Korea Institute of Ceramic Engineering & Technology 233-5 Gasan-dong Geumcheon-gu 153-801 Seoul, South Korea

*Corresponding author: Fax: +82 32827769; Tel: +82 32822427; E-mail: cykim15@kicet.re.kr

AJC-11355

In this study, the porous series of carbon aerogel (CA) by a magnesium acetate catalyst molar ratio, CA50, CA100, CA200 and CA500, were derived *via* the pyrolysis of resorcinol-formaldehyde (RF) aerogel. Pore structure analysis shows that a magnesium acetate ratio is increasing with decreasing a pore and particle size by FESEM. Surface area analysis is increasing with increasing a catalyst ratio by nitrogen adsorption/desorption analysis. The results show that BET surface area and specific capacitance increase with decreasing R/C ratio (molar ratio of resorcinol to catalyst). The BET surface area of carbon aerogel decreases from 763 m^2/g for CA50 to 523 m^2/g for CA500. The micropore volume are almost same for carbon aerogels, but the mesopore volume and specific surface area decreased with increasing R/C ratio, especially drastically decreased for CA500. The macropore volume decrease is not so high, about 0.3 cc/g from 2.3 cc/g for CA50 to 2.0 cc/g for CA500, indicating that CA500 is mainly comprised of macropores and micropores. To measure the real supercapacitance of carbon aerogels, we measured full-cell galvanostatic charge and discharge properties and cyclic voltammetry (CV) properties. The calculated capacitance of supercapacitors 24.5 F/g for CA50, 21.9 F/g for CA100, 11.3 F/g for CA200 and 4.5 F/g for CA500. We found that specific capacitance is increasing with increasinga surface area and large amount of mesopores.

Key Words: Carbon aerogel, Supercapacitor, Pore structure, Specific surface area, Mesopore.

INTRODUCTION

Carbon aeorlgels (CAs) are new ultralight materials with many interesting properties, such as low mass densities, continuous porosities, high surfaces and high electrical conductivity[1-10]. These properties are derived from the aerogel microstructure, which is a network of interconnected primary particles with characteristic diameters between 3 and 33 nm. Supercapacitance is different from the battery which is used the chemical reaction to produce the electric energy from an oxidation/de-oxidation reaction. The principles of electric generation in battery is a chemical reaction, the principles of electric energy generation in electric double-layer capacitor is physical adsorption. The prior products was used the inorganic electrolyte below 1F capacitance with low consumer current like μA in memory back up power. Though a continuous development and research, the various materials are invented. After using the organic electrolyte, the energy density is improved because of the rated voltage is increased until 2.5 V.

Recently, supercapacitors have been considered as a promising a high power energy source for digital communication, high power suppliers, memory bank up systems and advanced vehicles, *e.g.*, hybrid electric and fuel cell vehicles[11-24]. Although they cannot store as much energy as batteries, supercapacitors possess advantages such as higher charge/discharge efficiency, longer cycle life and faster charge capability. In conclusion, we can control the pore size and specific surface area and pore volume by varying R ratio. We can obtain very nanoporous carbon aerogel materials by adding magnesium acetate upto 50 of R ratio. CA50 has high specific surface area and pore volume including micropores, mesopores and macropores, so that it has the highest specific capacitance value, 25 F/g for full cell.

EXPERIMENTAL

Synthesis of carbon aerogel: Resorcinol-formaldehyde aerogels were prepared in an aqueous solution of resorcinol (R) and formaldehyde (F) with a molar ratio of 1:2[25]. We used magnesium acetate [$Mg(CH_3COO)_2$] as a catalyst with various catalyst concentrations (referred to as R/C at, molar ratio) to prepare a series of carbon aerogel with solid content of 40 wt %. Resorcinol (99 %, Yakuri pure chemicals Co. Ltd.), formaldehyde (Fluka, 36.5 % in water, methanol-stabilized) and magnesium acetate tetrahydrate (Fluka, 99.5 %) were dissolved in deinoized water under magnetic stirring to obtain a homogeneous solution. After curing (1 day at room temperature, 1 day at 298 K and

†Presented to The 5th Korea-China International Conference on Multi-Functional Materials and Application.

2 days at 333 K), the wet gels were immersed in acetone to exchange the water inside the pores, then dried at 40 ºC under super critical pressure, further pyrolyzed at temperature of 1073 K under a nitrogen atmosphere to obtain carbon aerogels. The samples were denoted as CA_{40x}, where 40 means a solid content of 40 wt % and x indicates the catalyst concentration.

Preparation of supercapacitor electrode: To prepare the electric double-layer capacitor (EDLC) electrode, a mixture of the prepared carbon, carbon aerogel (active material), acetylene black (conductivity enhancing material), polytetrafluoroethylene (PTFE-60 wt % binder) were dispersed in isopropyl alcohol. The mass ratio carbon aerogel/acetylene black/ binder was 9:0.5:0.5 to form slurries. On the other hand, the sheet type electrode kneaded with PTFE was bonded with a conductive adhesive on a titanium plate. The carbon aerogel (2 cm diameter) was putted on a piece of titanium plate (127 μm thickness) by a graphite conductive adhesive.

Electrochemical measurement: The ions of electrolyte cannot penetrate completely into the micropore, which leads to a poor utilization of surface area[25]. Correspondingly, carbon aerogel spheres combining enhanced mesoporosity with well-developed pore interconnectivity would yield a promising potential for the application in electrode materials for an electric double-layer capacitor[26]. The influence of pore structure in the above carbon materials on a capacitive behaviour was investigated. The charge-discharge cycling tests in a three-electrode cell with 2M H_2SO_4 electrolyte and a Ag/AgCl reference electrode (half cell) at the current 1 mA/cm^2. During charging, a constant charge current of 3.14 mA was supplied to electric double-layer capacitor until a full-charge voltage of 1.0 V was built up. During discharging, the electric double-layer capacitor discharges through an electronic load at a constant discharge current of 3.14 mA. The specific capacitance of carbon aerogel electrodes for supercapacitor was determined on a capacitance measurement cell using a typical galvanometric charge/discharge method. Before the measuring, carbon aerogel electrodes were immersed in a 2M H_2SO_4 electrolyte for 1 day to make the electrolyte completely diffuse into the pores. The most common techniques for estimating the capacitance are the following: cycle voltammetry [I = f(E)] and galvanostatic charge/discharge method was used to carry out the electrochemical measurement. As electrochemically inert current collectors, 99.9 % titanium plates were used. The electrochemical measurements (cyclic voltammetry and electrochemical impedance analysis) were carried out in a three electrode cell using carbon coated on a titanium plate as the working electrode with a graphite sheet and a saturate calomel electrode (SCE) as the counter and the reference electrode, respectively. Two carbon aerogel electrodes were separated by a 0.1 mm thick microporous polypropylene membrane and an electrolyte solution. Before measurement was made, the carbon aerogel electrodes were placed in the 2M sulfuric acid electrolyte solution for 1 day to ensure complete filling of the porous electrodes. This assembly was placed in a Teflon cell containing 2M sulfuric acid electrolyte solution as the electrolyte. To calculate the specific capacitance, this cell was charged with a constant current 3.14 mA/s until 1 V and discharged with constant current -3.14 mA/s to 0 V. The specific capacitance of a single carbon aerogel electrode was calculated from this charge/discharge curve using eqn. 1.

$$C = \frac{I\Delta t}{\Delta V m} \quad (1)$$

where C is the specific capacitance (F/g), I is the constant current, Δt is the time period, ΔV is the potential difference and m is the mass of the carbon aerogel electrode, using a AUTO-LAB (PGASTA12). All the measurements were carried out at room temperature. The specific capacitance (C_{st}) of the electrode at different scanning rates in a 2M sulfuric acid electrolyte solution as the electrolyte was estimated from the following equation[26]

$$C_{st} = \frac{I_a + [I_c]}{2m(dV/dt)} \quad (2)$$

where I_a, I_c, m and dV/dt are the current of on positive and negative sweeps, mass of the active materials and the sweep rate, respectively. The Ragone plots are frequently used in demonstration of power densities and energy densities of supercapacitors. The energy density (in Wh/kg) is calculated as[27].

$$E = \frac{1}{2}CV^2 \quad (3)$$

where C is the capacitance of the two-electrode capacitors and V is the voltage decrease in discharge. The power (P in W/kg) is calculated as

$$P = \frac{2E}{\Delta t} \quad (4)$$

where E is the energy density and Δt is the time spent in discharge[27].

RESULTS AND DISCUSSION

Gelation of resorcinol and formaldehyde: FT-IR spectra of resorcinol-formaldehyde (RF) aerogels, RF50, RF100, RF200 and RF500 synthesized by supercritical drying of resorcinol-formaldehyde gels were shown in Fig. 1(a). For resorcinol-formaldehyde gels, OH stretching and CH_2 stretching modes appeared at 2935 and 3385 cm^{-1}. An aromatic C=C stretching absorption band at 1605 cm^{-1} is considered to be related to the double bond of resorcinol. The bands at 1218 and 1085 cm^{-1} are attributed to CH_2-O-CH_2 formed *via* polycondensations of resorcinol and formaldehyde. It indicates that the formation of chains by resorcinol and formaldehyde reactions and the chains linked each other to generate clusters and then the clusters forms resorcinol-formaldehyde gel network structures. However, we cannot find any difference between resorcinol-formaldehyde aerogels with different catalyst quantities.

FT-IR spectra of carbon aerogels with different magnesium acetate catalyst ratio were shown in Fig. 1(b). For carbon aerogel gels, the OH stretching and CH_2 stretching modes appeared at 3451 and 2917 cm^{-1}. FT-IR data showed that the lesser the quantity of catalyst, magnesium acetate, the higher the intensity of OH stretching band. It means that water adsorption quantity is higher in carbon aerogels 50. It is because the pore size is bigger than another carbon aerogels, as is shown in the electron microscopy and nitrogen adsorption and desorption analysis results. The band at 1625 cm^{-1} is assigned to CH_2 bending modes. After carbonization, an aromatic C=C stretching at 1605 cm^{-1} disappeared. Raman scattering from the carbon aerogel scattered by 532 nm laser light are shown in

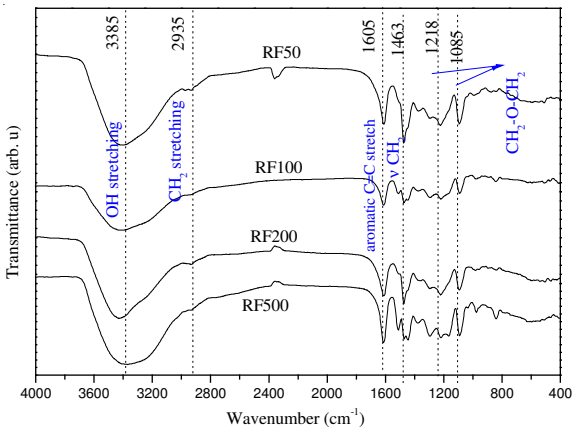

(a)

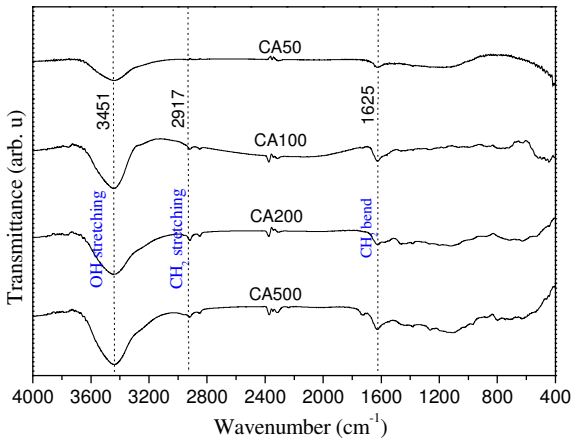

(b)

Fig. 1. FT-IR transmittance spectra of resorcinol-formaldehyde aerogel (a) and carbon aerogel (b)

Fig. 2. The Raman peaks showed 1586 and 1342 cm^{-1}, which is attributed to carbon. The first peak is considered to be attributed to D-band at 1350-1290 cm^{-1} from defective graphite. The second peak is thought to be G-band (graphite) at 1588-1545 cm^{-1}. D band at 1314 cm^{-1} of CA50 is very broader and G band intensity is a little larger than that of D band. It is thought that graphite structure is better developed than another carbon aerogels, which showed almost same intensities of D and G band.

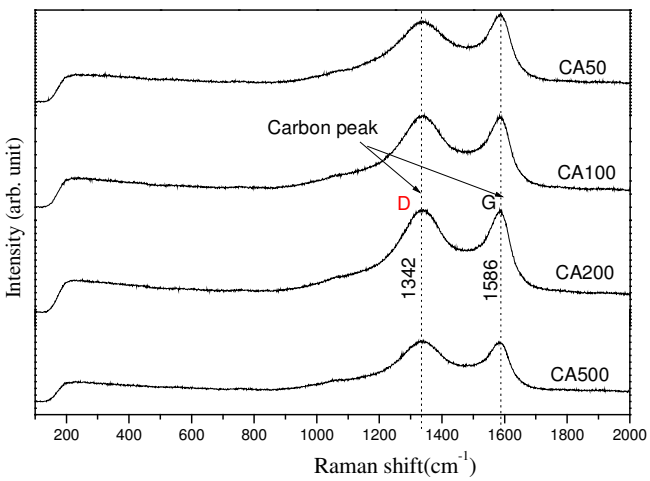

Fig. 2. An spectra of the produced carbon aerogel

Fig. 3 shows the X-ray diffraction patterns of carbon aerogel by magnesium acetate catalyst ratio. The XRD patterns show amorphous carbon and for CA50, the XRD peaks showed the pattern of graphite patterns. It indicates that CA50 is comprised of nanocrystalline and amorphous carbon phases. Magnesium acetate prompted to link the chains of resorcinol-formaldehyde and form very nanoporous network structures, which affect the different patterns of CA50.

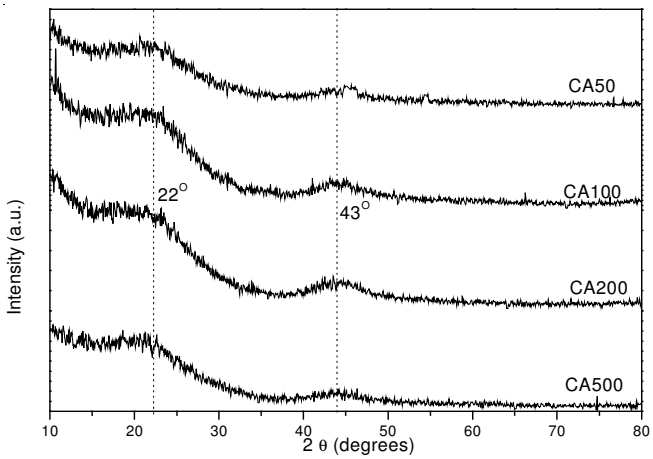

Fig. 3. X-Ray diffraction spectra of carbon aerogel

Microstructures of carbon aerogels: The specific surface areas of the carbon aerogels are calculated by using the (Brunauer-Emmett-Teller) BET model equation in N_2 adsorption-desorption analysis. As shown in Fig. 4(a), the shapes of the hysteresis loop of the carbon aerogels are characteristically different with magnesium acetate catalyst ratio changed. The isotherms of CA50 showed type IV, typical of mesoporous structure. The adsorbed nitrogen gas volume of CA50 is linearly increased with relative pressure until 0.80 and then increased abruptly and reached to the maximum cumulative volume, 650 cm^3/g at near saturated pressure during absorption process. The maximum nitrogen gas adsorption volume of CA100, CA200 and CA500 are 445, 296 and 174 cc/g, respectively. It means that CA50 is higher mesoporous and microporous materials. The pore volume decreased with increasing resorcinol-formaldehyde/catalyst ratio. Therefore, the quantities of catalyst are one of the important factors to form link and cluster of resorcinol-formaldehyde and then 3-dimensional gel networks of clusters. The more catalyst is considered to generate the more mesoporous networks of carbon aerogels. During desorption process, liquified nitrogen in the pores was dissociated to generate nitrogen gas and the cumulative absorbed volume decreased greatly in the region of 0.80-1 of P/P_o for CA50, CA100 and CA200. For CA500, the region of great desorption change shifted to 0.45-1 of P/P_o. It indicates that the CA500 is comprised of smaller sized pores, compared to those of CA50, CA100 and CA200.

The pore size distribution is shown in Fig. 4(b). The pore diameter of CA50 is 14-33.9 and 18.9-63.9 nm for CA100, 14.5-33.4 no for CA200 and 1.8-3.8 nm for CA500. The pore size distribution is almost same for CA50, CA100 and CA200, in the range of 15-60 nm. However, the pore size became the smallest value, few nanometer below 4 nm. CA500 did not show type IV characteristics of isotherms and its pore volume

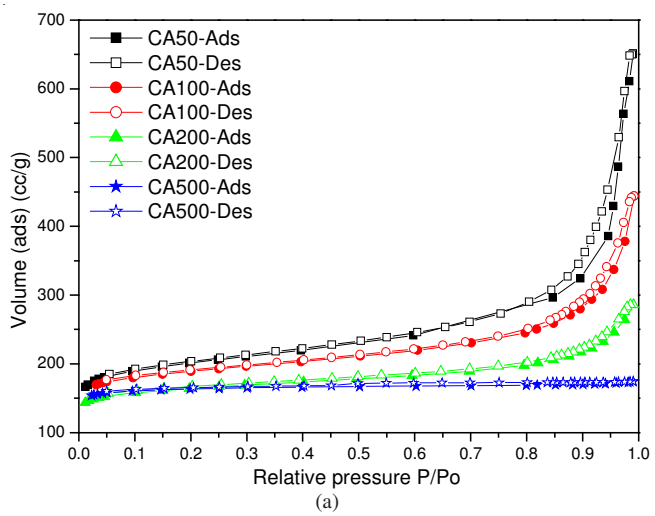

(a)

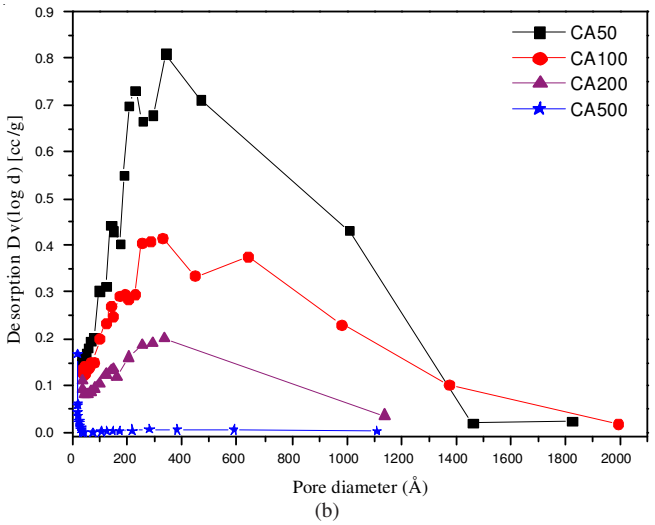

(b)

Fig. 4. Nitrogen adsorption isotherms for Vads (a) and the pore size distributions calculated by BJH method in N_2 desorption (b)

is very small. It is considered that the small catalyst ratio per resorcinol-formaldehyde for CA500 is not enough to form mesoporous cluster networks, so that it did not show mesoporous characteristics of isotherms. The specific surface area of CA50 aeriel is 763 m^2/g and decreases to 725, 642 and 523 m^2/g for CA100, CA200 and CA500, respectively. The apparent density of CA50 aeriel is 0.248 g/cc and increases to 0.267 and 0.320 and 0.320 g/cc for CA100 and CA200 and CA500, respectively. The porosity of carbon aerogel decreases from 83 for CA50 to 78 % for CA500. The mesopore volume is 0.749 cc/g for CA50 and decreased to 0.427 cc/g for CA500 (Table-2).

Fig. 5 shows SEM images of carbon aerogels. It was observed the samples of CA50, CA100 and CA200 are comprised of about 10 nm-sized nanoparticles and clusters of nanoparticles. It is considered that micropores exist between nanoparticles and mesopores were in inter-clusters. Macropores above few hundred nanometers were also observed. CA500 showed a little different image. The primary particle size is about 1 μm and the conglomerations of the primary particles formed few-micron sized clusters and therefore, there is no mesopores but macropores with few microns. The microstructures of carbon aerogels were detailed in TEM images in Fig. 6. CA50 is comprised of about few nanometers to 10 nm sized particle networks with about few and 10 nanometer sized pores. The primary particle size increased with increasing resorcinol-formaldehyde/catalyst ratio, about 10-20 nm diameter. Therefore, CA100 and CA200 are comprised of 10-20 nm sized mesopores and hundred nanometer sized mesopores. CA500 aerogel consisted of large carbon sheet with 10-20 nm sized small pores and macropores were also observed between the sheet clusters with few micron size.

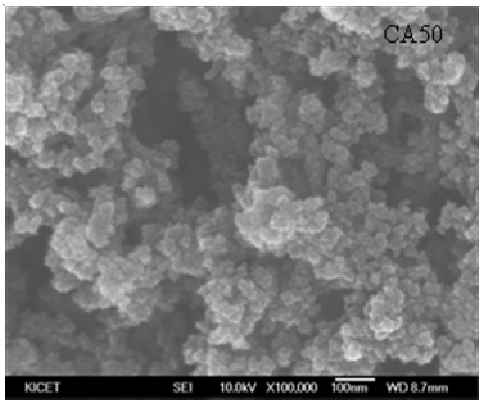

TABLE-1
RESORCINOL-FORMALDEHYDE BASED CARBON AEROGEL (CA) PRECURSORS

Sample	Materials					
	Resorcinol (mol)	Formaldehyde (mol)	H_2O (mol)	$Mg(OAc)_2 4H_2O$ $\times 10^{-4}$ (mol)	Resorcinol/ $Mg(OAc)_2 4H_2O$	Resorcinol (%)
CA50	0.145	0.29	3.33	29.0	50	40
CA100	0.145	0.29	3.33	14.5	100	40
CA200	0.145	0.29	3.33	7.25	200	40
CA500	0.145	0.29	3.33	2.90	500	40

TABLE-2
CARBON AEROGEL CATALYST RATIO PROPERTY

Sample	Item						
	BET (m^2/g)	Pore volume (cc/g)			Pore size (Å)	Density (g/cm^3)	Porosity (%)
		V_{meso}	V_{micro}	V_{macro}			
CA50	763	0.749	0.253	2.380	338.9	0.248	83
CA100	725	0.427	0.258	2.440	328.0	0.267	83
CA200	642	0.217	0.218	2.070	334.5	0.320	81
CA500	523	0.042	0.234	2.030	38.2	0.320	78

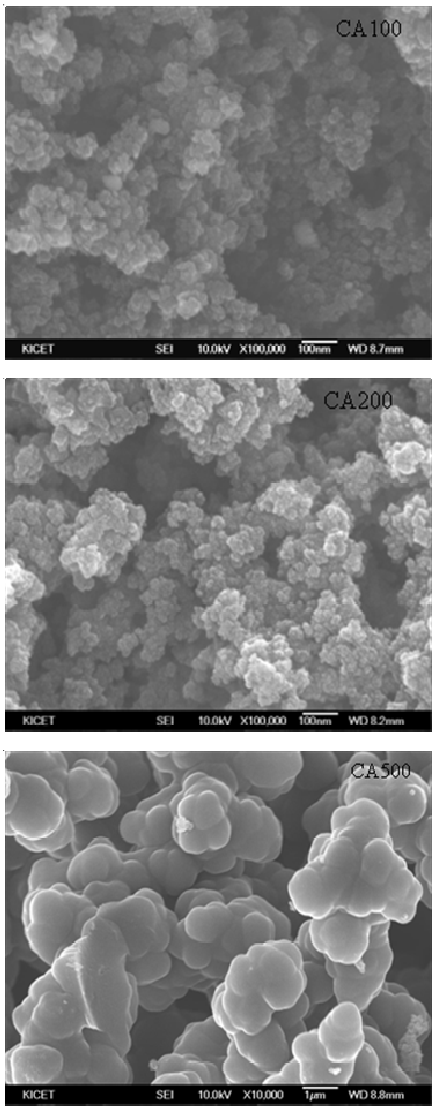

Fig. 5. FE-SEM image of carbon aerogel (CA)

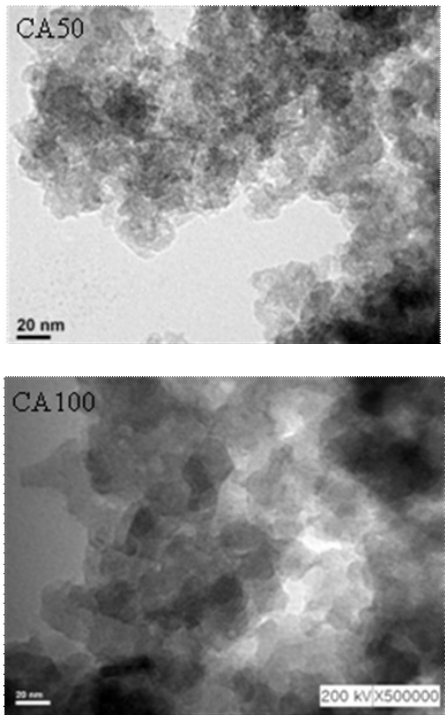

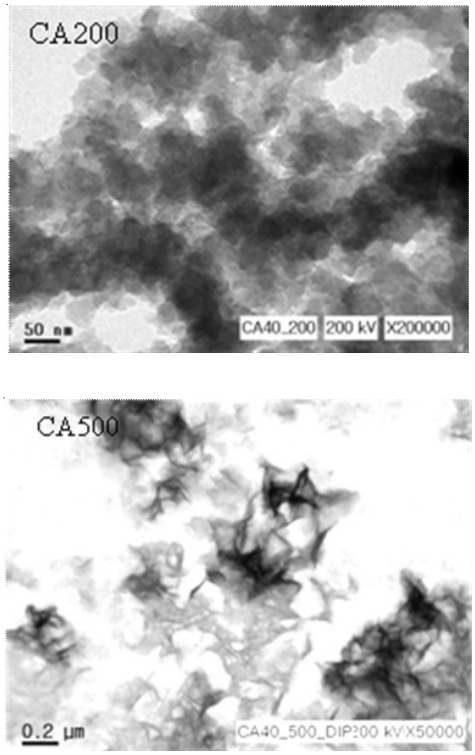

Fig. 6. TEM image of carbon aerogel (CA)

Electrochemical properties of carbon aerogel: The half-cell galvanostatic charge/discharge curves of carbon aerogels electrodes measured at a current of 3.14 mA are shown in Fig. 7(a). The voltage changes of carbon aerogels electrodes with time variations during charge and discharge occurred *via* two steps, with an inflection point at around 0.5 V. It is guessed that the two step charge and discharge is caused by the surface oxidation states of carbon aerogels. The calculated capacitance of supercapacitors of carbon aerogels by eqn. 1 is shown in Fig. 7(b). The half-cell specific capacitance of CA50 electrodes is 125.1 F/g, which is 28 times larger than that of CA500 electrode, 4.4 F/g. The specific double layer capacitance is stored in the double layers of carbon aerogels so that we need a large specific surface area and high porous materials to make proton ions or lithium ions approach and forms double layers, that is, high supercapacitance. As mentioned in our previous nitrogen absorption and desorption and microstructures analyses of carbon aerogels, CA50 showed the highest pore volume and the largest specific surface area. However, the ratio of the specific surface area of CA50 to CA500 is not so high, 1.46 times as high as that of CA500. The pore volume of CA50 is 0.75 cm^3/g about 5 times as high as that of CA500, 0.14 cm^3/g. The higher half-cell specific capacitance of CA50 than anticipated is considered to result from pseudocapacitance from the oxidation and reduction of carbon aerogels. Therefore, it has no practical meaning for the application of supercapacitors. Fig. 7(b) showed the supercapacitance variations with current. In the measurement of galvanostatic charge and discharge suepercapacitance, current density is very important. As is shown in Fig. 7, the higher capacitance value was obtained when we charge or discharge with the lower current density.

The CV curves are also shown in Fig. 8(a). In the CV curves, oxidation and reduction peak appeared at around 0.5-

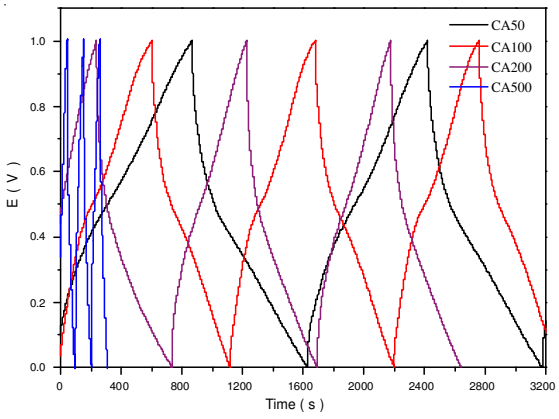

(a)

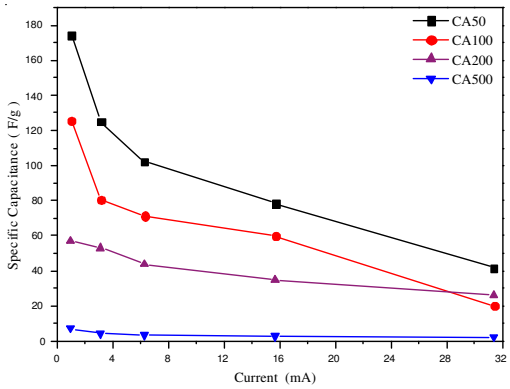

(b)

Fig. 7. Charge/discharge curves of carbon aerogel aerogel at current of 1 mA/cm^2 in half cell (a) and specific capacitance of the supercapacitor estimated from charge/discharge in half cell (b)

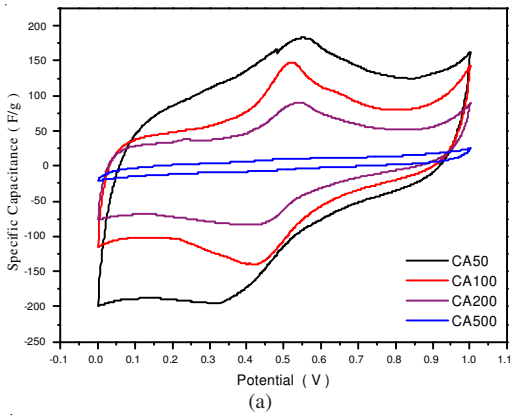

(a)

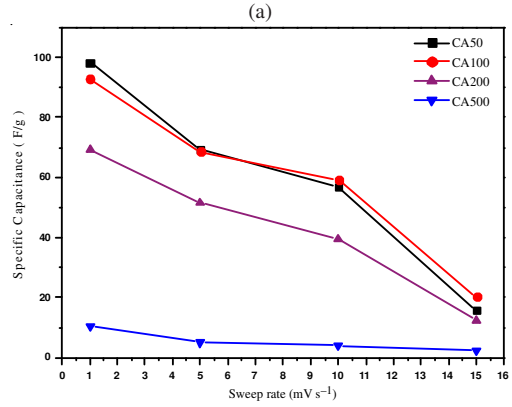

(b)

Fig. 8. Cycle voltammetry of characteristic of electrodes at scan rate of 1 mV/s in half cell (a) specific capacitances of carbon aerogel electrodes at scan rate from cyclic voltammetry in half cell (b)

0.6 and 0.3-0.6 V. Carbon aerogels with the more catalyst ratio per resorcinol-formaldehyde showed the larger CV hysteresis curves and the peak of oxidation shifted higher voltage to 0.6 V and the reduction peak lowered to 0.3 V. This phenomenon is almost true for CV analysis of carbon aerogels. When we measure the CV properties of carbon aerogels with lower sweep rate, we obtained the large CV curves as is shown in Fig. 8(b). The half-cell supercapacitance properties are summarized in Table-3. To measure the real supercapacitance of carbon aerogels, we investigated full-cell galvanostatic charge and discharge properties and CV properties of carbon aerogels [Fig. 9(a-b)]. The calculated capacitance of supercapacitors is 24.5 F/g for CA50, 21.9 F/g for CA100, 11.3 F/g for CA200 and 4.5 F/g for CA500. As is shown in Fig. 9(a), the galvanostatic charge and discharge curves showed the different behaviour from those of half-cell carbon aerogels electrodes.

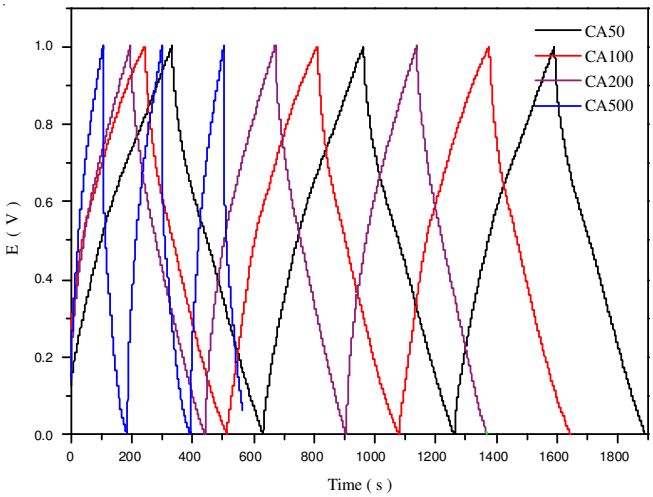

(a)

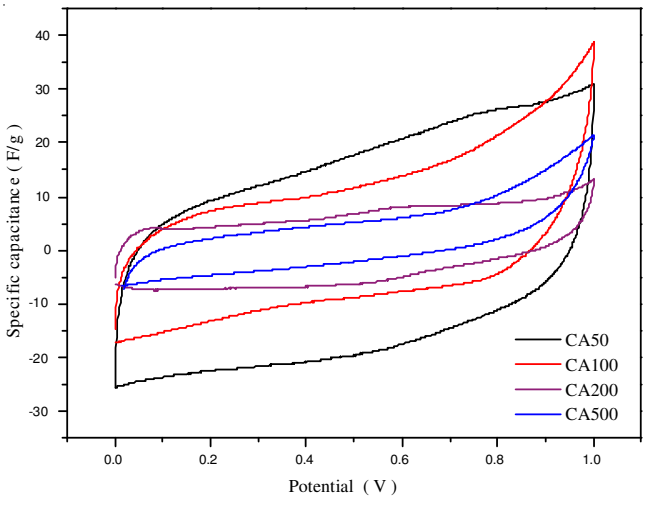

(b)

Fig. 9. Charge/discharge curves of carbon aerogel at current of 1 mA/cm^2 in full cell (a) and cycle voltammetry of characteristic of electrodes at scan rate of 1 mV/s in full cell

These results showed that half-cell supercapacitance showed the higher capacitance value. At the present, there is no precise cause, but it is guessed that the higher electrical voltage is applied when half-cell test is conducted, 1.3 V of real electrical potential for 1 V of nominal potential. Therefore,

TABLE-3
ELECTROCHEMISTRY PROPERTIES OF CA AEROGELS IN HALF CELL AND FULL CELL

Sample		Item					
		Capacitance		ESR(Ω)		Energy density (Wh/kg)	Powder density (W/kg)
		F (g)	F (cc)	10 (kHz)	1 (kHz)		
Half cell	CA 40/50	125.1	41.7	0.1547	0.2376	17.4	165.7
	CA 40/100	80.2	36.0	0.1817	0.2904	11.1	155.0
	CA 40/200	52.9	29.9	0.1703	0.2762	7.4	105.8
	CA 40/500	4.4	12.4	0.1738	0.3560	0.6	78.6
Full cell	CA 40/50	24.5	8.8	0.0755	0.1993	3.4	82.3
	CA 40/100	21.9	7.9	0.1195	0.2799	3.0	78.2
	CA 40/200	11.3	6.4	0.1253	0.3467	2.1	64.1
	CA 40/500	4.5	3.4	0.1456	0.3251	0.6	48.2

it is right to adopt full-cell supercapacitance value as a real value. The specific capacitance value of CA50 is about 4 times as high as CA500. This is higher than anticipated from BET specific surface area ratio, 1.4 times as high as CA500. The supercapacitance value is closely related with the pore size and volume as well as specific surface area of carbon aerogels. As is shown in Fig. 9(b), full-cell CV curves of carbon aerogels showed very small oxidation and reduction peaks. As mentioned before, it is because the higher electrical potential is applied when we charge or discharge in the half-cell test. When the resorcinol-formaldehyde/catalyst ratio was decreased, the carbon aerogel sample showed higher specific surface area and pore volume, so the CV curve had larger hysteresis loop, compared with another carbon aerogels synthesized using the smaller catalyst, magnesium acetate. The full-cell supercapacitance properties are summarized in Table-3.

Impedance spectroscopy is a useful technique for the measurements of capacitance giving complementary results. Fig. 10 presents the impedance spectra of carbon aerogels between 100-10 mHz. These loops are described elsewhere as a pseudo-transfer resistance[13] and associated with the porous structure of electrode. We analyzed the impedance properties of carbon aerogels samples. As is seen in Table-2, the quantity of catalyst for synthesis of resorcinol-formaldehyde gel affects the pore structures of carbon aerogel samples. Double layer capacitance values decreased with decreasing the quantities of catalyst; the value decreased from 3.916×10^{-4} F for CA50 to 1.526×10^{-4} F for CA500. The parallel resistance of CA50 was 0.6617 Ohm and decreased to 0.3574 Ohm for CA100 and 0.3714 Ohm for CA200 and then increased greatly to 3.014 O hm for CA500. The decrease of the resistance for CA100 and CA200 is considered to be related to the increase of the densities compared to that of CA50. The decrease of catalyst quantity made the amorphous carbon granule size large and the pore volumes small. However, the great increase of the resistance for CA500 is thought to result from the great size of carbon granules and the large pore size, so that the transport of carrier electrons between large carbon granules is very difficult. It is guessed from the impedance curve shapes that the pore structures of CA50, CA100 and CA200 is comprised ball-shape pores (4 type) and diagonal shape pores (2 types) for CA500.

Conclusion

We found that magnesium acetate contents are very important to form chains, clusters and cluster networks of

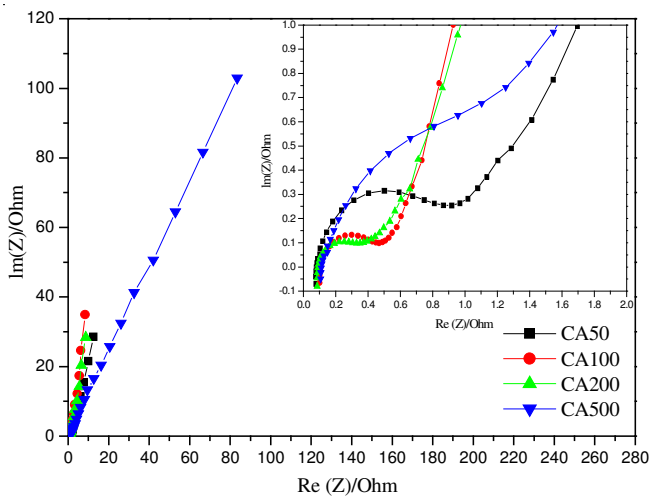

(a)

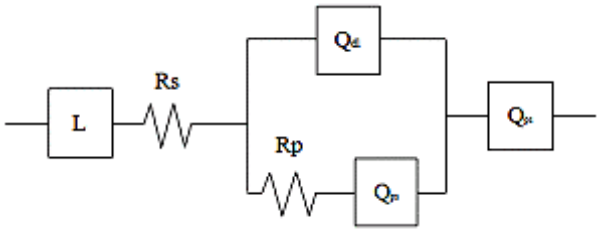

(b)

Fig. 10. Nyquist plots for 3.14 cm^2 cells assembled with electrodes containing carbon aerogel In 100 kHz-10 mHz (a) and and their equivalent circuit (b)

TABLE-4
DOUBLE LAYER CAPACITANCE AND PARALLEL RESISTANCE OF CAS

Samples	C_{dl} (× 10_{-4} F)	R_p (Ohm)
CA50	3.916	0.6617
CA100	3.867	0.3574
CA200	2.957	0.3714

formaldehyde-modified resorcinol. The contents more than 200 of ratio form highly mesoporous networks, but macroporous networks below 200 are generated. Nitrogen adsorption and desorption analyses and Archimedes measurement showed that carbon aerogels are comprised of micropores, mesopores and macropores. The micropore volume are almost same for carbon aerogels, but the mesopore volume and specific surface area decreased with increasing R ratio, especially drastically decreased for CA500. The macropore volume decrease is not

so high, about 0.3 cc/g from 2.3 cc/g for CA50 to 2.0 cc/g for CA500, indicating that CA500 is mainly comprised of macropores and micropores. Electrochemical analyses show that carbon aerogels with smaller R ratio show good capacitance value, which is considered to result from and the large specific surface area, large mesopores and the decrease of ESR or resorcinol-formaldehyde.

REFERENCES

1. New Electronics www.neon.co.uk 28 March, pp. 25-26 (2006).
2. Supercapacitors, US DoE overview, www.doe.org
3. H. von Helmholtz, *Ann. Phys. (Leipzig)*, **89**, 211 (1853).
4. N.D. Lang and W. Kohn, *Phys. Rev*., **B1**, 4555 (1970); **B3**, 1215 (1971).
5. G. Gouy, *Ann. Phys., Paris*, **7**, 129 (1917); *J. De Phys*., **9**, 457 (1910).
6. O. Stern, *Z. Elektrochem*., **30**, 508 (1924).
7. R.W. Pekala, *J. Master. Sci*., **24**, 3221 (1998).
8. W. Li, G. Reichenauer and J. Fricke, *Carbon*, **40**, 2995 (2002).
9. G.X. Wang, L. Yang, S.L. Bewlay, Y. Chen, H.K. Liu and J.H. Ahn, *J. Power Sources*, **146**, 521 (2005).
10. E. Guilminot, F. Fischer, M. Chatenet, A. Rigacci, S. Bethon-Fabry, P. Achard and E. Chainet, *J. Power Sources*, **166**, 104 (2007).
11. R.W. Pekala, C.T. Alviso, F.M. Kong and S.S. Hulsey, *J. Non-Cryst. Solids*, **145**, 90 (1992).
12. R.W. Pekala, J.C. Farmer, C.T. Alviso, T.D. Tram, S.T. Mayer, J.M. Miller and B. Dunn, *J. Non-Cryst. Solids*, **225**, 74 (1998).
13. E. Frackowiak and F. Beguin, *Carbon*, **39**, 937 (2001).
14. Y.Z. Wei, B. Fang, S. Iwasa and M. Kumagai, *J. Power Sources*, **141**, 386 (2005).
15. X.Y. Wang, X.Y. Wang, W.G. Huang, P.J. Sebastian and S. Gamboa, *J. Power Source*, **140**, 211 (2005).
16. W.G. Pell and B.E. Conway, *J. Power Sources*, **63**, 255 (1996).
17. L. Matos, S. Fernandes, L. Guerreiro, S. Barata, A.M. Ramos, J. Vital and I.M. Fonseca, *Micropor. Mesopor. Master*, **92**, 38 (2006).
18. M. Itagaki, S. Suzuki, I. Shitande, K. Wantanabe and H. Nakazawa, *J. Power Sources*, **164**, 415 (2007).
19. W.R. Li, D.H. Chen, Z. Li, Y.F. Shi, Y. Wan, G. Wang, Z.Y. Jiang and D.Y. Zhao, *Carbon*, **45**, 1757 (2007).
20. X. Andrieu, G. Crepy and L. Josset, In: Proceedings of the 3rd International Seminar on Double Layer Capcaitors and Similar Energy Storage Devices, Florida Educational Seminar, December (1993).
21. Y.Z. Wei, B. Fang, S. Iwasa and M. Kumagai, *J. Power Sources*, **141**, 386 (2005).
22. J. Randin and E. Yeager, *J. Electroanal. Chem*., **36**, 257 (1972).
23. L. Meyer, *Trans. Faraday Soc*., **34**, 1056 (1938).
24. R.F. Strickland-Constable, *Trans. Faraday Soc*., **34**, 1074 (1938).
25. V. Sihvonen, *Trans. Faraday Soc*., **34**, 1062 1938).
26. R. Schilow, *Zeit. Phys. Chem*., **149**, 211 (1930).
27. J.D. Lambert, *Trans. Faraday Soc*., **34**, 1080 (1938).